PERGAMON

Water Research 36 (2002) 5102–5112

WATER RESEARCH

www.elsevier.com/locate/watres

Linking biokinetics and consumer–resource dynamics of zinc accumulation in pond abalone *Haliotis diversicolor supertexta*

Chung-Min Liao[a,*], Ming-Chao Lin[b], Jui-Sheng Chen[c], Jein-Wen Chen[a]

[a] *Department of Bioenvironmental Systems Engineering, National Taiwan University, Taipei, Taiwan 10617, ROC*
[b] *Life Science Division, General Education Center, Nanhua University, Chiayi, Taiwan, ROC*
[c] *Department of Environmental Engineering and Sanitation, Foo-Yin Institute of Technology, Kaohsing, Taiwan 831, ROC*

Received 16 May 2001; received in revised form 30 April 2002; accepted 20 May 2002

Abstract

A dynamic model that links biokinetics and consumer–resource dynamics for describing zinc (Zn) accumulation in abalone *Haliotis diversicolor supertexta* has been developed and then applied to Zn data from real abalone farms. The biokinetic parameters used in this study, uptake and depuration rate constants of abalone and their food source, red alga *Gracilaria tenuistipitata* var. *liui*, were obtained from a laboratory 14-d exposure experiment. We carried out a sensitivity analysis of the model by using the fractional factorial design technique, taking into account the influence of consumer–resource-related parameters such as growth and death rates and biomass and biokinetic parameters characterized by bioconcentration factor. Results indicate that the response time of biomagnification dynamics of Zn accumulation in abalone was influenced mainly by the growth rate of algae and biomass and the death rate of abalone and by interactions algae biomass and abalone death rate and abalone and algae biomass. New algae production results in substantially higher values of biomagnification factor. The linked model was then applied to field observations from a real-life situation of variable Zn concentrations occurring in abalone farms. Simulation results show that the predicted values are within a factor of 2 of the measured values (% errors range from $5.3 \pm 4\%$ to $44.1 \pm 8\%$). Both model analysis and model application to the abalone farms suggest that the linking influences between biokinetics and consumer–resource dynamics support Zn accumulation in *H. diversicolor supertexta* and in *G. tenuistipitata* var. *liui* as functions of Zn concentration in water and abundance of food occurring in abalone farms.

Keywords: Abalone; Algae; Bioaccumulation; Consumer–resource dynamics; Zinc

1. Introduction

Abalone are common gastropod molluscs that inhabit the coastal reefs in tropical and subtropical areas [1]. The herbivorous gastropod, *Haliotis diversicolor supertexta*, is the most abundant abalone species in Taiwan. The red alga *Gracilaria tenuistipitata* var. *liui* is the major forage for culturing the abalone *H. diversicolor supertexta*. These two species are commercially important for fisheries and aquaculture in Taiwan [2]. *H. diversicolor supertexta* is also appreciated for its delicacy and high market value, the aquaculture of *H. diversicolor supertexta* thus is a promising business [2,3]. However, the coastal regions of Taiwan where the abalone and algae aquaculture facilities are located are subjected to polluted discharges from rivers.

Zinc (Zn) is an essential micronutrient found at high levels in the algae and in the tissues of fish/shellfish [4,5]. Zinc is available to abalone from both the dissolved phase (e.g., gill uptake) and the diet (e.g., algae ingestion). If waterborne Zn levels are elevated, however, toxicity can occur and have severe effects on the

*Corresponding author. Tel.: +886-2-2363-4512; fax: +886-2-2362-6433.
E-mail address: cmliao@ccms.ntu.edu.tw (C.-M. Liao).

0043-1354/02/$ - see front matter
PII: S0043-1354(02)00230-0

health of abalone, which will reduce the market price and cause closure of abalone farms [1,6,7]. Previous investigations indicated that Zn have been detected in many rivers in that maximum Zn concentrations in contaminated aquacultural waters are reported to range from 60 to 300 $\mu g\,L^{-1}$ in different areas of Taiwan [8]. At these levels, Zn specifically disrupts calcium uptake by the gills [9,10], leading to hypocalcemia, which may end with the death of the fish within a few days, depending on the Zn concentration.

Abalone/algae uptake and consumer–resource interactions are the two most relevant processes affecting the fate of waterborne Zn in aquacultural ecosystems. Abalone/algae uptake is the first step in the bioaccumulation of waterborne Zn in aquacultural food webs and also plays a major role in the occurrence and biogeochemical cycles of Zn in the aquatic environments.

Bioconcentration occurs by means of passive diffusion of waterborne metals from the ambient water via gills into circulatory fluid and then deposition in the tissues, whereas biomagnification is the transfer of metals from lower trophic level to higher trophic level [11–13]. Therefore, bioconcentration of toxic metals in consumer biomass through uptake represents a "top-down" disturbance, whereas biomagnification showing the alteration of resource availability represents a "bottom-up" perturbation of aquatic ecosystems. An understanding of how bottom-up and top-down processes influence the dynamics of aquacultural communities is necessary for effective management of aquacultural ecosystems in the face of environmental variability and multiple human impacts. It is difficult, however, to determine the effects of resource availability and food webs interactions in open highly variable aquacultural systems.

To assess the feeding and growth rates that influence metals accumulation to the abundance of resources and consumers, we adopted the consumer–resource model from population biology, incorporating the bioaccumulation model to make quantitative predictions about the effects. There are a number of observations regarding the occurrence of waterborne metals in aquatic food webs in pristine environments that suggest that bioaccumulation kinetics and consumer–resource dynamics are linked [14–17].

The objectives of the present paper are to study the mutual influences between biokinetics and consumer–resource dynamics of Zn accumulation in *H. diversicolor supertexta* and to determine whether consumer–resource dynamics can support Zn concentrations observed in real abalone farms. A model for linking biokinetics and consumer–resource dynamics is developed, allowing the linkages between abalone/algae uptake and population-dynamic component of the system to be elucidated. We conducted a 14-d laboratory exposure experiment to determine the biokinetic parameters from bioconcentration and depuration bioassays. The integrated bioaccumulation–consumer–resource model will then be applied to field data collected from real abalone farms located in different sites of Taiwan region in order to determine whether it can describe Zn concentrations in abalone and algae as a function of Zn concentration in pond water and the abundance of food occurring in those farms.

2. Experiments

2.1. Sampling, acclimation and exposure conditions

The most important farming areas for the production of abalone *H. diversicolor supertexta* are in Toucheng on the north coast, Kouhu on the western coast, and Anping on the south cost of Taiwan. All the abalone farms use seawater from polluted coastal areas. Thus we collected the samples of the abalone, the algae *G. tenuistipitata* var. *liui* and ambient water from nine farms in the three locations mentioned above. Three abalone, three algae and three 500 mL water samples per site were collected. The abalone and algal samples initially were washed in seawater to remove epiphytes and kept at 4°C during transfers to the laboratory. The water samples were fixed by adding 5 mL 1 N HNO_3.

Living abalone *H. diversicolor supertexta*, and the alga *G. tenuistipitata* var. *liu*i were collected from Toucheng for the laboratory exposure experiments, because this place was the most Zn-contaminated area of the three sites. Abalone with a shell length of 4 cm were selected for the experiments. The algal samples selected were mature, whole and healthy. An amount of 200 abalone was transferred into four aquatic tank of approximately 54 L volume, containing 50 L of artificial seawater. In order to imitate the environment of the abalone farms, the abalone were held in baskets. Each tank contained 10 baskets. Four abalone per basket were used for analysis. To assure that at least four abalone would be alive at the end of the experiment, we put one extra abalone in each basket. Dissolved oxygen was maintained close to saturation by aeration throughout the experiment. The temperature was maintained at 25 ± 1.5°C under constant illumination [18]. The salinity was maintained at 35. The pH remained fairly constant during the assays (7.75 ± 0.24). Abalone were fed daily with *G. tenuistipitata* var. *liui.* The abalone and algae were acclimatized for 2 weeks before they were exposed to Zn.

2.2. Bioconcentration and depuration assays

In two tanks Zn ($ZnCl_2$) was added to the seawater; in one tank the abalone were fed with algae (water/food-exposed), and in the other tank the abalone were kept

without food (water-exposed). The Zn contamination level was determined by a preliminary test exposing abalone to different Zn concentrations of 0.25, 0.5, 1, 2, 4, and 6 mg L^{-1}. The median lethal tolerance (LT_{50}) of abalone at $\leqslant 1$ mg L^{-1} Zn was longer than 21 d. Thus, the organisms were exposed to 1 mg L^{-1} Zn for 7 d. The algae and the abalone were reared in the contaminated environment for 7 d uptake, then transferred to clean seawater and reared for 7 d of depuration. To examine if starvation affects Zn depuration in abalone, the same procedure with abalone and algae was followed over 14 d using the other two tanks, but without Zn in the sea water.

Abalone, algae and water samples were collected at day 0, 1, 2, 4, and 7, starting from the day the organisms were exposed to the contaminated seawater and from the day the organisms were transferred to clean seawater. Every time we took one basket along with 500 mL water out of each tank. From this basket four pieces of algae and four abalone were collected. Because preliminary observation showed that *H. diversicolor supertexta* only feeds at night and has empty gut in the evening, we collected the abalone at night to make sure the contents of gut would not influence the results. The experiments in the four tanks, described above, were repeated again. The water samples were fixed with 5 mL 1 N HNO_3, and the samples of abalone were stored in the dark at -20°C until they were analyzed.

2.3. Metal analysis

The algae and dissected abalone were freeze-dried overnight, and then grounded to a fine powder in a grinder (Tai-Hsiang S36-89, Taiwan). The 500 mg portions of the ground samples were digested in 10 mL of 65% concentrated HNO_3 (v/v) overnight at room temperature. The resulting solution was evaporated and redissolved in 0.1 N HC1 [19]. Zinc analysis was carried out by atomic absorption spectrophotometry using a Perkins Elmer model 5000 atomic absorption flame spectrophotometer equipped with a graphic furnace. The detection limit was 5 μg Zn/L water and 0.5 μg Zn/g tissue. External quality control was achieved by digesting and analyzing identical amounts of rehydrated (90% water) standard reference materials (DORM-2, Dogfish Liver-2-oganic matrix, provided by the NRC-CNRC, National Research Council Canada). Recovery rates ranged from 95% to 97%.

2.4. Data analysis

Bioconcentration is assumed to follow a well-established first-order one-compartment model as $dC_b/dt = k_{1b}C_w - k_{2b}C_b$ in that the solution at the constant C_w is $C_b(t) = C_b(t=0) + \mathrm{BCF}\, C_w(1 - e^{-k_{2b}t})$ (referred to as the UD model), where C_b is the Zn concentration in biota (μg g^{-1}), C_w is the Zn concentration in water (dissolved phase) (mg L^{-1}), k_{1b} is the uptake rate constant from dissolved phase by biota (L g^{-1} d^{-1}), k_{2b} is the depuration rate constant for Zn in biota (d^{-1}), and BCF (mL g^{-1}) is a general equilibrium bioconcentration factor that is calculated as $\mathrm{BCF} = k_{1b}/k_{2b} = C_b/C_w$. Equilibrium biomagnification factor of abalone (BMF_m) was calculated from the concentration of the Zn accumulated in the abalone (C_m) divided by the Zn concentration in the algae (C_a) as $BMF_m = C_m/C_a$.

The k_{1b} s and k_{2b} s that characterizes Zn bioconcentration/depuration process in *H. diversicolor supertexta* and *G. tenuistipitata* var. *liui* contaminated from food and water can be estimated by nonlinear regression fitting the UD model to the measured Zn concentration data from the 7-d uptake experiments. The depuration rate constants (k_{2b} s) can also be calculated by the linear regression of log-transformed tissue Zn concentration on depuration days from the 7-d depuration experiments as $\ln C_b(t) = \ln C_b(t=T) - k_{2b}t$, where T is the time when depuration begins. Variances in k_{2b} s derived from two methods were tested for homogeneity using an F-test. Values were then compared using t-test.

All curve fittings were performed using the nonlinear regression option of the Statistica® software (StatSoft, Tulsa, OK, USA). The Statistica® was also used to calculate the coefficient of determination (r^2) and statistical analyses (analysis of variance and Student's t-test).

3. Mathematical model

3.1. Model description

Traditional predator–prey models are introduced in the original models of Lotka [20] and Volterra [21]. It has been refined in a number ways, notable via the introduction, by Holling [22,23], of the notion of a predator functional response. The basis of much predator–prey theory will have the structure

$$\frac{dN}{dt} = f(N)N - g(N,P)p, \tag{1}$$

$$\frac{dP}{dt} = \varepsilon g(N,P)P - \mu P, \tag{2}$$

where N denotes the prey density, P the predator density, $f(N)$ the per capita prey growth rate in the absence of predators, and $g(N,P)$ the rate at which an individual predator consumes prey. The function $g(N,P)$ is the functional response of the model. The parameter ε describes the efficiency of the predator in converting consumed prey into predator offspring, whereas μ is the predator mortality rate. The functional response in

Eqs. (1) and (2) is said to be Holling type II prey dependent if $g(N,P) = g(N)$.

The assumptions underlying in our approach are that (i) the algae satisfy a logistic growth function and (ii) the functional response of the model follows the Holling type II function in that the saturation effect affects the functional response of the abalone to change in the algae density.

In our notation, the derivation in Eqs. (1) and (2) yields a consumer–resource dynamics of abalone and algae:

$$\frac{dA(t)}{dt} = r_a\left(1 - \frac{A(t)}{K}\right)A(t) - g\left(\frac{A(t)}{A(t)+D}\right)M(t), \quad (3)$$

$$\frac{dM(t)}{dt} = fg\left(\frac{A(t)}{A(t)+D}\right)M(t) - \mu_m M(t), \quad (4)$$

where r_a is the growth rate of algae (d^{-1}), K is the algae carrying capacity ($g\,L^{-1}$), $A(t)$ is the algae biomass as a function of time t ($g\,L^{-1}$), $M(t)$ is the abalone biomass as a function of time t ($g\,L^{-1}$), D is the half-saturation for algae ingestion ($g\,L^{-1}$), f is the biomass conversion efficiency of ingested algae (dimensionless), g is the grazing rate of algae by abalone ($g\,g^{-1}\,d^{-1}$), and μ_m is the abalone death rate (d^{-1}). The $(A/(A+D))M$ terms can also be thought of as representing the conversion of energy from one source to another: $g(A/(A+D))M$ is taken from the algae and $f\ g(A/(A+D))M$ accrues to the abalone.

The scenario that we considered is (i) the exchange of Zn between abalone and dissolved Zn was modeled as a first-order process, with additional Zn accumulation from ingested algae, (ii) abalone ingest only algae and other suspended particles, bacteria and detritus uptakes are negligible, (iii) tissue concentration of Zn per unit biomass of abalone increases as a result of direct uptake from water and through assimilation of contaminated algae, and (iv) tissue concentration tend to decrease as a result of elimination from the whole body and growth dilution.

The dynamic model describing the Zn accumulation in abalone and algae can be expressed by reconsidering from the viewpoint of consumer–resource dynamics in Eqs. (3) and (4) as

$$\frac{dC_m(t)}{dt} = \left(k_1 + k_{1f}\left(\frac{A(t)}{A(t)+D}\right)BCF_a\right)C_w - \left(k_2 + k_{2f} + fg\left(\frac{A(t)}{A(t)+D}\right)\right)C_m(t), \quad (5)$$

$$\frac{dC_a(t)}{dt} = k_{1a}C_w - \left(k_{2a} + k_{1f}\left(\frac{M(t)}{A(t)}\right)BMF_m\right)C_a(t), \quad (6)$$

where $C_m(t)$ is the time-dependent Zn concentration in abalone soft tissue ($\mu g\,g^{-1}$), t is the time of exposure (d), C_w is the dissolved Zn concentration in water ($\mu g\,g^{-1}$), k_1 is the uptake rate constant from dissolved phase by abalone ($mL\,g^{-1}\,d^{-1}$), k_{1f} is the uptake rate constant from algae by abalone ($g\,g^{-1}\,d^{-1}$), BCF_a is the bioconcentration factor for Zn in algae ($mL\,g^{-1}$), k_2 is the depuration rate constant for Zn in abalone (d^{-1}), k_{2f} is the depuration rate constant for Zn from food in abalone (d^{-1}), $C_a(t)$ is the time-dependent Zn concentration in algae ($\mu g\,g^{-1}$), k_{1a} is the uptake rate constant from dissolved Zn by algae ($mL\,g^{-1}\,d^{-1}$), k_{2a} is the depuration rate constant for Zn in algae (d^{-1}), and BMF_m is the biomagnification factor for Zn in abalone (dimensionless).

3.2. Numerical issues

The system of Eqs. (3)–(6) is a nonlinear, first-order system of coupled differential equations. Integration over time is straightforward in principle but is complicated by existence of a large number of widely differing time scales. The numerical integration scheme used to solve the system dynamic Eqs. (3)–(6) is a subroutine DIVPRK based on the Runge–Kutter–Verner 5th-order and 6th-order method that is provided by IMSL Subroutines Library [24] and done in double precision with FORTRAN 90. The algorithm is stable provided the error and the convergence criteria are carefully monitored. We used numerical scheme to solve Eqs. (3)–(6) under a number of biokinetic parameters obtained from 14-d exposure experiment and field data from nine abalone farms as well as parameters related to feeding rate and population dynamics, which are estimated in the following section.

3.3. Values used in consumer–resource dynamic model

The values of the parameters used in the consumer–resource dynamic model are indicated in Table 1. Some more important parameters will be discussed briefly below. Properties such as biomass conversion efficiency for ingested algae, algae growth rate, abalone death rate and grazing rate of algae by abalone were directly adopted from the literature. Certain other parameters that could not be easily measured have been estimated and, in some cases, the influence has been tested varying their values in the model simulations. The estimated parameters are the algae carrying capacity and half-saturation biomass for algae ingestion.

Algae carrying capacity (K): Typical growth rates for algae are around 0.01–0.04 $g\,g^{-1}\,d^{-1}$, corresponding to instantaneous growth rates of 0.005–0.026 [25]. Preliminary simulations showed that grazing at realistic zooplankton biomass had little effect on algae biomass. We therefore used the observed long-term average algae biomass of $150 \pm 14\,g\,L^{-1}$ (ranging from 90 to 210 $g\,L^{-1}$) [26] as an approximation to algae carry capacity.

Half-saturation biomass for algae ingestion (D): The determination of half-saturation biomass for algae

Table 1
Parameters values (mean ± s.d.) used in the consumer–resource dynamic model

Parameter	Symbol	Value
Initial abalone biomass	M_i ($g\,L^{-1}$)	Varied
Initial algae biomass	A_i ($g\,L^{-1}$)	Varied
Dissolved Zn	C_w ($\mu g\,g^{-1}$)	Varied
Growth rate of algae	r_a (d^{-1})	0.038 ± 0.013[a]
Grazing rate of abalone	g ($g\,g^{-1}\,d^{-1}$)	0.25 ± 0.05[b]
Biomass conversion rate for algae ingested by abalone	f ($g\,g^{-1}$)	3.50 ± 0.81[b]
Death rate of abalone	μ_m (d^{-1})	0.286 ± 0.17[c]
Algae carrying capacity	K ($g\,L^{-1}$)	150 ± 14.2[b]
Half-saturation for algae ingestion	D ($g\,L^{-1}$)	61[d]

[a] Adopted from Lee et al. [25].
[b] Adopted from Chen and Lee [26].
[c] Adopted from Shepherd [27]: at age 8 months to 4 years.
[d] Estimated by fitting Eqs. (3) and (4) to field observations.

ingestion, D, can be approximately obtained by fitting the Holling type II function of Eqs. (3) and (4) with the known values of grazing rate of abalone (g), death rate of abalone (μ_m) and growth rate of algae (r_a) given in Table 1, to the biomass observations for algae and abalone collected from abalone farms in Toucheng area. The resulting value is $D = 61\,g\,L^{-1}$.

4. Results

4.1. Results of 14-d exposure experiments

The uptake and depuration rate constants used in this study were obtained from laboratory experiments designed to maintain constant Zn concentration in the water in order to properly apply the UD model and to treat them mathematically. Fig. 1 shows the results from the exposure experiments of Zn in soft tissue of *H. diversicolor supertexta* and in algae *G. tenuistipitata* var. *liui*. The nonlinear regression equations resulting from the best fits of the UD model to data of uptake and depuration phases of Zn by abalone (Fig. 1A) were for food exposed, $C(t) = 111 + 180.40(1 - e^{-0.636t})$ ($r^2 = 0.99$) and for water exposed, $C(t) = 111 + 166.01(1 - e^{-0.611t})$ ($r^2 = 0.98$). Fig. 1B shows the uptake/depuration experiment results of Zn by algae in that the optimal fit to the data results in a nonlinear regression equation of $C(t) = 98.3 + 163.9(1 - e^{-0.588t})$ ($r^2 = 0.98$).

A simple UD model was thus successfully fitted by the nonlinear technique to the uptake/depuration curves of the 14-d exposure data in that coefficients of determination generally were high ($r^2 > 0.95$). Results suggest that

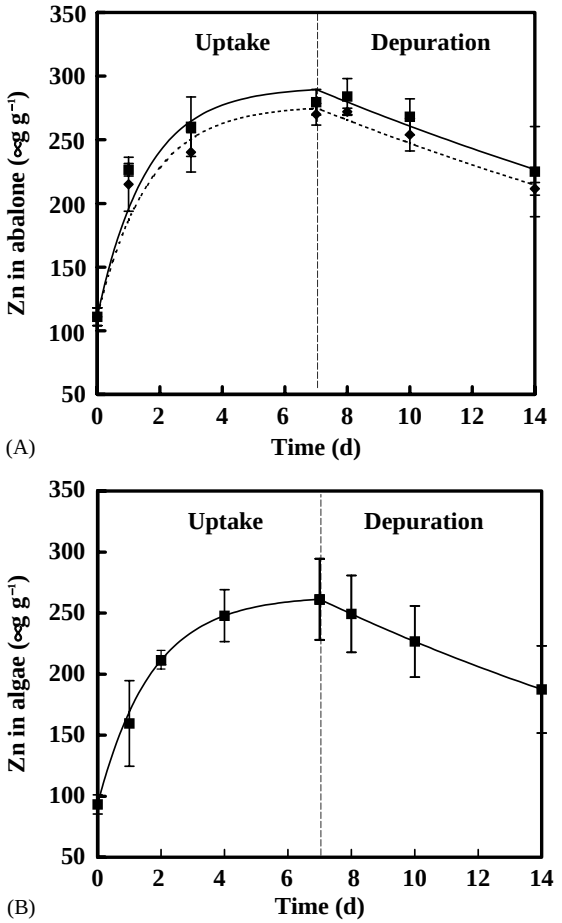

Fig. 1. Laboratory 14-d exposure experiment results: (A) uptake and depuration of Zn by soft tissue of *H. diversicolor supertexta* during a 7-d exposure and then a 7-d depuration period. The measurements (mean ± s.d.) are shown with symbols ((■) fed with algae; (◆) kept without algae); and the model fittings are shown in lines ((—) fed with algae; (- - -) kept without algae) and (B) uptake and depuration of Zn by algae *G. tenuistipitata* var. *liui* during a 7-d exposure and then a 7-d depuration period. The measurements (mean ± s.d.) are shown with symbols and the model fitting is shown in solid line.

the fitted first-order equation is an appropriate model for the data set. Estimates of k_2 and k_{2f} were also determined from the depuration-phase experiments (Fig. 1). All of these regressions were significant ($p < 0.05$), with r^2 values that ranged from 0.7 to 0.85. The k_2 and k_{2f} values determined in depuration experiments were also statistically significant ($p < 0.05$) from their corresponding k_2 and k_{2f} values derived from nonlinear curve fitting the UD model to the uptake data. Table 2 summarizes the experimentally determined biokinetic parameters for the UD model describing Zn

bioaccumulation process in *H. diversicolor supertexta* and *G. tenuistipitata* var. *liui* contaminated by Zn from food and water.

4.2. BMF dynamics

A typical example of the dynamic simulation carried out for the dynamics of algae and abalone biomass and Zn concentrations in algae and abalone is shown in Fig. 2. The Zn concentration in algae attained a steady state by the end of the simulation, whereas the Zn concentration in abalone increased rapidly up to day 3 then decreased and attained a steady state by the end of the simulation (Fig. 2A). Fig. 2B indicates that over 30 d, algae biomass decreased rapidly but abalone biomass increased slightly and has a peak occurring at day 5. Fig. 3 illustrates the BCF_a and BMF_m dynamics, showing the response times toward 95% equilibrium during the simulation. The Zn concentration in algae increases with time and couples the whole Zn bioaccumulation process of water–algae–abalone in that BCF_a increases with time and reach equilibrium much shorter than that of BMF_m which decreases with time (Fig. 3).

Table 2
Experimentally determined values (mean ± s.e.) of uptake rate constants and depuration rate constants for the UD model describing Zn bioaccumulation process in abalone and algae contaminated from food and water

	Uptake rate constants
Abalone	
Foof-exposed	$k_{1f} = 113.84 \pm 24.4$ ($g\,g^{-1}\,d^{-1}$)
Water-exposed	$k_1 = 102.04 \pm 23.2$ ($mL\,g^{-1}\,d^{-1}$)
Algae	$k_{1a} = 100.1 \pm 22.8$ ($mL\,g^{-1}\,d^{-1}$)
	Depuration rate constants
Abalone	
Food-exposed	$k_{2f} = 0.636 \pm 0.21$ (d^{-1})
Water-exposed	$k_2 = 0.611 \pm 0.43$ (d^{-1})
Algae	$k_{2a} = 0.588 \pm 0.23$ (d^{-1})

5. Discussion

5.1. Sensitivity analysis

The 2^k factorial optimization, an experimental design approach, was used for sensitivity analysis. Factorial design allows the determination of the effects of different variables and their interactions with a minimum number of runs [28,29]. Interactions of three or more variables are usually negligible and/or hard to interpret; therefore, a fractional factorial design was used. Details on factorial experimental design and their applications to sensitivity analysis can be found elsewhere [30–33].

All the variables related to biokinetic properties are considered as one variable since they cannot be modified independently. This variable will be the bioconcentration factor for Zn in algae (BCF_a) since this biokinetic parameter can be expressed as the ratio between the

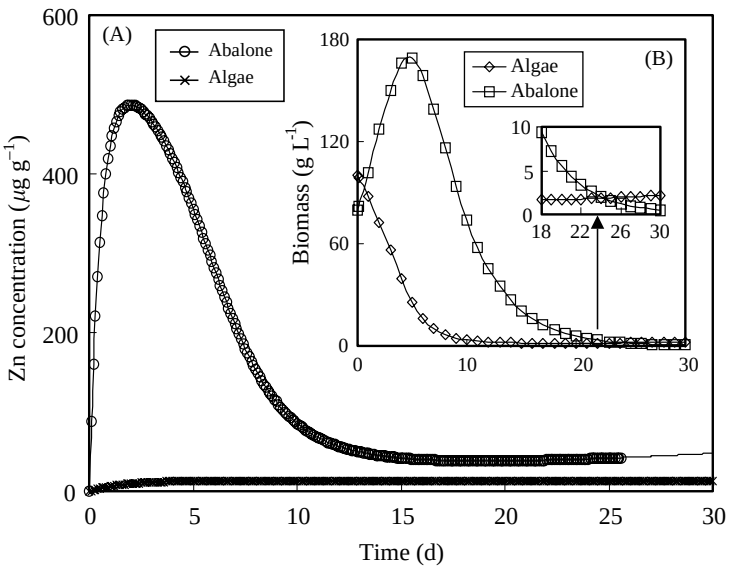

Fig. 2. Typical example of the simulations carried out for the model predictions of (A) Zn concentration in algae and abalone and (B) biomass of algae and abalone. The initial conditions used were as: $C_w = 80\,\mu g\,L^{-1}$, $A(0) = 100\,g\,L^{-1}$, $M(0) = 80\,g\,L^{-1}$, equilibrium $BCF_a = 167$, and equilibrium $BMF_m = 1.8$.

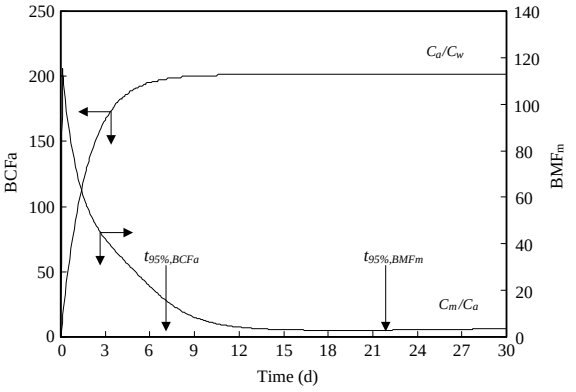

Fig. 3. Typical example of the simulation carried out for BCF_a and BMF_m dynamics, showing an approach to 95% equilibrium response time for BCF_a ($t_{95\%,BCF_a}$) and BMF_m ($t_{95\%,BCF_a}$). The initial conditions used were as: $C_w = 80\,\mu g\,L^{-1}$, $A(0) = 100\,g\,L^{-1}$, and $M(0) = 80\,g\,L^{-1}$.

equilibrium conditions of Zn concentration in algae and Zn concentration in water. In addition to different BCF_a values, we accounted for biomass of algae and abalone, algae growth rate, abalone grazing rate, and abalone death rate. With six variables (Table 3), a full factorial design requires 64 (2^6) experiments. With fractional factorial design the sensitivity analyses can be performed with 32 (2^{6-1}) runs of the model. Table 3 shows data from a complete 2^5 fractional factorial design for the 32 runs of the sensitivity analysis of the model. The time to reach 95% of equilibrium for the BMF_m dynamics was chosen as the response time since the dynamics of this processes can be compared independent of the initial conditions (Fig. 3). The time required to reach 95% of equilibrium of BMF_m ($t_{95\%,BMF_m}$) is the response time of the system to changing Zn concentration accumulation in abalone. Response times for equilibrium BMF_m dynamics are listed in Table 3.

The effect of each variable on the response was determined using the following equation [28]:

$$\begin{aligned} t_{95\%,BMF_m} = {} & aA + bM + cr_a + dg + e\mu_m + fBCF_a \\ & + hAM + iAr_a + jAg + kA\mu_m + lABCF_a \\ & + mMr_a + nMg + oM\mu_m + pMBCF_a \\ & + qr_a g + rr_a\mu_m + sr_a BCF_a + tg\mu_m \\ & + ugBCF_a + v\mu_m BCF_a + w, \end{aligned} \quad (7)$$

where $a-w$ are the parameters obtained by fitting the response times by multiple linear regression. The Student's t-test of these parameters allowed the determination of significance of each variable and the interactions between variables [28,33]. The significant variables with a confidence level higher than 95% are (a) the main effects: algae growth rate (r_a), abalone biomass (M), and abalone death rate (μ_m) and (b) the interactions: algae biomass/abalone death rate ($A\mu_m$), abalone biomass/algae biomass (MA), and algae growth rate/abalone death rate ($r_a\mu_m$). Response times for biomagnification dynamics of abalone are dependent on algae growth rate as well as biomass and death rate of abalone in a complicated way since they are interacting. Therefore, algae growth rate as well as biomass and death rate of abalone explain the majority of the variability of the abalone Zn accumulation dynamics, whose correlation coefficient was also significant.

No significant effect of Zn concentration in water was observed, although the importance of uptake kinetics for the higher Zn concentration in water has been reported. Explanation for this could be that the differences in uptake kinetic properties among different Zn concentrations in water are not sufficient to provide significantly different response times. The higher Zn in water, however, may have very different uptake dynamics. A second complementary sensitivity analysis was performed for Zn in water and modifying all other variables one at a time. This allowed the determination of interactions between different Zn concentrations in water and the variables related to abundance of food in determining the 95% equilibrium BMF_m values. Fig. 4 shows that 95% of equilibrium BMF_m values were affected by the growth rate and the biomass of algae. Higher values of BMF_m were obtained for higher growth rate of algae. The effect on the BMF_m due to increasing algae biomass depends on the growth rate, which led to lower values of BMF_m at constant biomass (zero growth rate) and larger BMF_m values for higher growth rates.

Higher growth rates yield higher BMF_m values since new biomass needs to reach equilibrium with the dissolved Zn concentration in water. Fig. 4 also implies that higher algae biomass in the absence of algae growth depletes the water Zn concentration faster, achieving lower equilibrium BMF_m values. When the algae biomass is increasing ($r_a > 0$), however, response time of BMF_m values achieving equilibrium are longer (Table 3) due to the equilibrium requirements of the new biomass introduced in the system. An important result of the present study is the influence of algae uptake of dissolved Zn on the biomagnification dynamics of abalone.

Higher BMF_m values are obtained for higher values of algae growth rate and lower algae biomass since the effects of algae biomass and growth rate depend on the dissolved Zn concentration in water (Fig. 4). Furthermore, a dramatic increase of BMF_m values was observed for r_a other than zero. Therefore, algae growth rate has such a big influence on BMF_m values that, for Zn in water with 10^2–10^3 order of magnitude, algae biomass remains the same (Fig. 4). Algae uptake of Zn concentration by new biomass induces a depletion of the water Zn concentration, retarding and even preventing the

Table 3
A 2^5 fractional factorial design for the runs of the sensitivity analysis of the model and response times obtained for achieving 95% of equilibrium for BMF_m ($t_{95\%,BMF_m}$)[a]

Run	M ($g\,L^{-1}$)	A ($g\,L^{-1}$)	r_a (d^{-1})	G ($g\,g^{-1}\,d^{-1}$)	μ_m (d^{-1})	BCF_a ($L\,g^{-1}$)	$t_{95\%,BMF_m}$ (d)
1	20	50	0.04	0.25	0.3	167	25.9
2	80	50	0.04	0.25	0	167	35.2
3	20	100	0.04	0.25	0	167	39.4
4	80	100	0.04	0.25	0.3	167	17.6
5	20	50	0	0.25	0	167	43.4
6	80	50	0	0.25	0.3	167	32.9
7	20	100	0	0.25	0.3	167	37.6
8	80	100	0	0.25	0	167	37.2
9	20	50	0.04	0.5	0	167	32.8
10	80	50	0.04	0.5	0.3	167	14.8
11	20	100	0.04	0.5	0.3	167	17.1
12	80	100	0.04	0.5	0	167	28.7
13	20	50	0	0.5	0.3	167	33.3
14	80	50	0	0.5	0	167	47.3
15	20	100	0	0.5	0	167	49.8
16	80	100	0	0.5	0.3	167	17.6
17	20	50	0.04	0.25	0.3	16.7	24.7
18	80	50	0.04	0.25	0	16.7	32.8
19	20	100	0.04	0.25	0	16.7	36.3
20	80	100	0.04	0.25	0.3	16.7	16.9
21	20	50	0	0.25	0	16.7	40.2
22	80	50	0	0.25	0.3	16.7	28.4
23	20	100	0	0.25	0.3	16.7	33.3
24	80	100	0	0.25	0	16.7	35.4
25	20	50	0.04	0.5	0	16.7	29.8
26	80	50	0.04	0.5	0.3	16.7	13.1
27	20	100	0.04	0.5	0.3	16.7	14.9
28	80	100	0.04	0.5	0	16.7	26.3
29	20	50	0	0.5	0.3	16.7	27.6
30	80	50	0	0.5	0	16.7	43.7
31	20	100	0	0.5	0	16.7	45.9
32	80	100	0	0.5	0.3	16.7	16.7

[a] Here, A is the algae biomass, M is the abalone biomass, r_a is the algae growth rate, g is the grazing rate of algae by abalone, μ_m is the abalone death rate, and BCF_a is the bioconcentration factor for Zn in algae.

achievement of equilibrium between the Zn concentration in abalone and in water.

5.2. Model application to abalone farms

The simulations were performed using measured concentrations of Zn in pond water (Table 4) as initial conditions. Then the measured equilibrium BCF_a and BMF_m values (Table 4) associated with experimentally determined biokinetic parameters (Table 2) were incorporated into the model. Other variables needed to perform the calculations were biomass of algae and abalone observed in abalone farms (Table 4) and parameters of consumer–resource dynamics (Table 1). Zn concentrations in the algae and abalone were predicted by the output of the model.

The comparison of the predicted Zn concentrations in algae and abalone with measured concentrations in nine abalone farms is given in Figs. 5 and 6, respectively. Calculations indicate that the coupled dynamic model predicts the measured Zn concentrations with average relative differences ranging from 17% to 55% in algae and from 1.3% to 47% in abalone, respectively, where the relative difference or errors were determined as, $\text{error} = |(C_{pred} - C_{obs})/C_{obs}| \times 100$, in which C_{obs} is the observation data and C_{pred} is the predicted concentration. The predicted values are always within a factor of 2 of the measured values and are thus within the expected accuracy of the model due to uncertainties in the system variables.

The coupled dynamic model predicts the measured Zn concentration in algae with average relative differences

of 44.1±8.4%, 25.7±7.9%, and 26.4±4.5% for abalone farms in Toucheng, Kouhu, and Anping, respectively (Fig. 5) and the average relative differences of 41.1±6.1%, 5.3±4.3%, and 22.9±12.3%, respectively, between the measured and predicted Zn concentrations in abalone for abalone farms in Toucheng, Kouhu, and Anping (Fig. 6). Simulation results show that the model accurately reflects the variations of Zn concentrations accumulation in algae and abalone, pointing out the importance of consumer–resource dynamics in real abalone farm when modeling the metal bioaccumulation process.

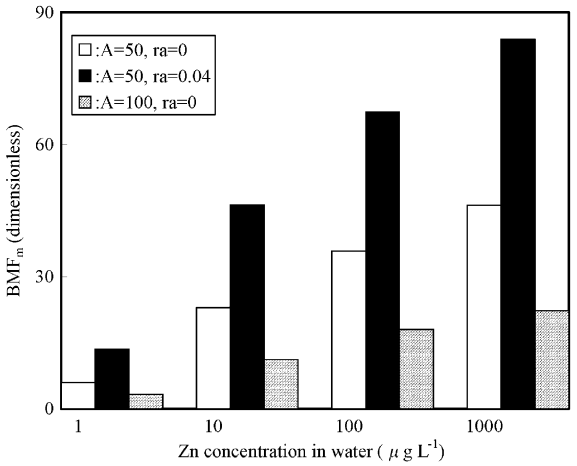

Fig. 4. Effects of algae biomass (A) and growth rate (r_a) depending on Zn concentrations in the water for the sensitivity analysis of 95% equilibrium BMF_m values.

Even though the simulations for the real abalone farms were using time-independent uptake and depuration rate constants for Zn accumulation in *H. diversicolor supertexta* and *G. tenuistipitata* var. *liui* obtained from a laboratory exposure experiment, an excellent fit between experimental observations and model outputs was obtained. This suggests that species allometric-dependent kinetic factor may play a secondary role in the interaction between abalone diets, population dynamics, and Zn accumulation.

The simulations suggest that some policy issues regarding water quality management in abalone farms may be reconsidered. The control of Zn loadings from polluted coastal areas is not a sufficient measure to control water Zn concentrations since trophic status plays a major role on the mid- and long-term pollution trends. Therefore, water quality management requires a multi-disciplinary approach. Water pollution issues must be addressed together with food web structure issues and account for the ecological complexity of the aquacultural environment.

6. Conclusions

The following conclusions can be drawn from this study:

1. Sensitivity analysis of the model indicates that the response time of biomagnification dynamics of Zn accumulation in abalone was influenced mainly by the growth rate of algae and biomass and the death rate of abalone and by interactions of algae biomass

Table 4
Measured values of dissolved Zn concentration in water (mean±s.d., $n = 3$), biomass of algae *G. tenuistipitata* var. *liui* and *H. diversicolor supertexta*, equilibrium binconcentration factor for Zn in algae (BCF_a), and equilibrium biomagnification factor for Zn in abalone (BMF_m) used in the simulations for nine abalone farms in Toucheng, Kouchu and Anping, respectively

Abalone farm	Zn in water (μg L^{-1})	Biomass (g L^{-1})		BCF_a (L g^{-1})	BMF_m (—)
		Algae	Abalone		
Toucheng					
Pond T-A	94.57±50.22	150	120	559	1.8
Pond T-B	144.17±32.48	180	100	757	1.1
Pond T-C	154.38±28.87	180	100	721	1.1
Kouhu					
Pond K-A	53.33±47.59	120	80	408	2.2
Pond K-B	85.03±11.72	120	120	260	2.4
Pond K-C	43.76±11.10	140	150	740	1.2
Anping					
Pond A-A	106.06±37.42	150	60	434	1.3
Pond A-B	57.75±12.60	140	60	503	1.6
Pond A-C	44.95±25.01	100	90	216	2.2

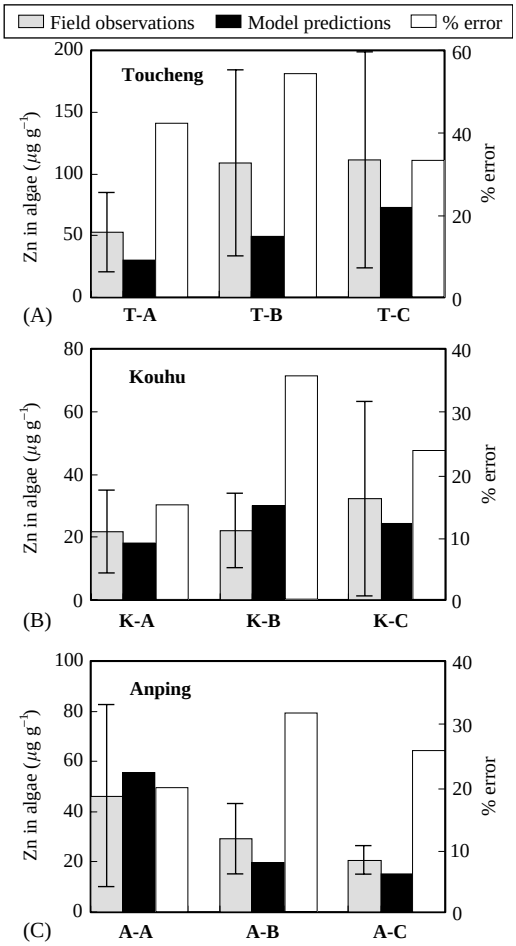

Fig. 5. A comparison between measurements (mean ± s.d., $n = 3$) collected from abalone farms of (A) Toucheng, (B) Kouhu, and (C) Anping and predictions for Zn concentration in algae *G. tenuistipitata* var. *liui*. The average relative differences (% error) are also shown.

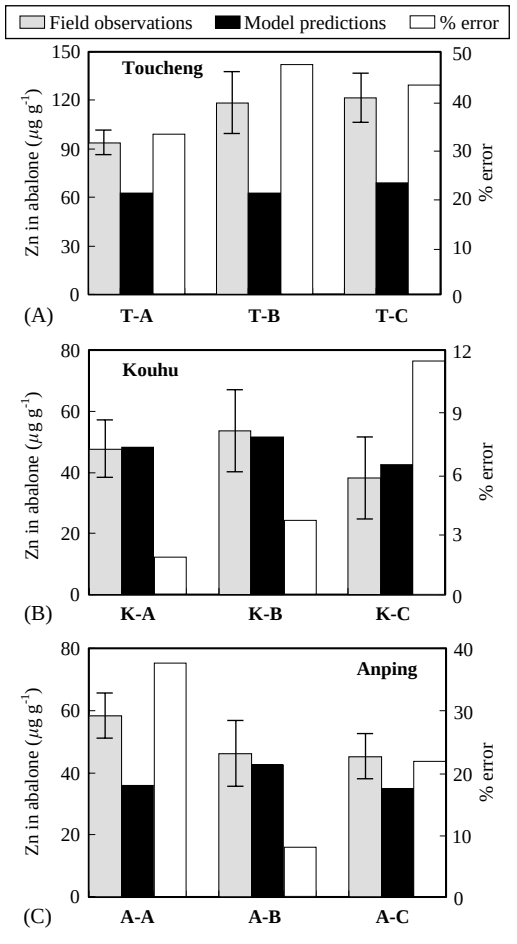

Fig. 6. A comparison between measurements (mean ± s.d., $n = 3$) collected from abalone farms of (A) Toucheng, (B) Kouhu, and (C) Anping and predictions for Zn concentration in abalone *H. diversicolor supertexta*. The average relative differences (% error) are also shown.

and abalone death rate and abalone and algae biomass.

2. New algae production results in substantially higher values of biomagnification factor of abalone. Algae uptake-induced depletion of Zn concentration maintains Zn concentration in abalone and in water out of equilibrium. The model results also point out the relevant role of algae, which is a dominant source of organic matter in abalone farms, in removal of Zn concentrations from polluted coastal areas by bioaccumulation process.
3. Model application to the abalone farms confirms our hypothesis that the consumer–resource dynamics effectively supports the Zn concentrations accumulation in algae and in abalone and suggests that bioaccumulation kinetics and consumer–resource dynamics are constrained by the same factors.

Acknowledgements

The authors would like to express their appreciation for the financial support of the National Science Council of Republic of China under Grant NSC 88-2313-B-002-070. The authors appreciate the contributive comments by anonymous referees. Sincere thanks also go to abalone farm owners for providing the valuable information and for the use of their abalone farms, without which this research work would have not been possible.

References

[1] Hahn KO. Biotic and abiotic factors affecting the culture of abalone. In: Hahn KO, editor. Handbook of culture of abalone and other marine gastropods. Boca Raton, FL, USA: CRC Press, 1989. p. 113–283.

[2] Chen HC. Farming the small abalone, *Haliotis diversicolor supertexta*, in Taiwan. In: Hahn KO, editor. Handbook of culture of abalone and other marine gastropods. Boca Raton, FL, USA: CRC Press, 1989. p. 265–83.
[3] Singhagraiwan T, Doi M. Seed production and culture of a tropical abalone *Haliotis asinine Linne*. Thailand: The Eastern Marine Fisheries Development Center, 1993. 31pp.
[4] Hogstrand C, Webb N, Wood CM. Covariation in regulation of affinity for branchial zinc and calcium uptake in freshwater rainbow trout. J Exp Biol 1998;201:1809–15.
[5] Genter RB, Lehman RM. Metal toxicity inferred from algal population density, heterotrophic substrate use, and fatty acid profile in a small stream. Environ Toxicol Chem 2000;19:869–78.
[6] Conroy PT, Hunt JW, Anderson BS. Validation of a short-term toxicity test endpoint by comparison with longer-term effects on larval red abalone. *Haliotis rufescens*. Environ Toxicol Chem 1996;15:1245–50.
[7] Knauer K, Behra R, Sigg L. Effects of free Cu^{2+} and Zn^{2+} ions on growth and metal accumulation in freshwater algae. Environ Toxicol Chem 1997;16:220–9.
[8] Lee CL, Chen HY, Chuang MY. Use of oyster, *Crassostrea gigas*, and ambient water to assess metal pollution status of the Charting coastal area, Taiwan, after the 1986 green oyster incident. Chemosphere 1996;33: 2505–32.
[9] Hogstrand C, Verbost PM, Bonga SEW, Wood CM. Mechanisms of zinc uptake in gills of freshwater rainbow trout: interplay with calcium transport. Am J Physico-Regulatory Integrative Comparative Physico 1996;39: R1141–7.
[10] Galvez F, Webb N, Hogstrand C. Zinc binding to the gills of rainbow trout: the effect of long-term exposure to sublethal zinc. J Fish Biol 1998;52:1089–104.
[11] Connell DW. Bioaccumulation of chemicals by aquatic organisms. In: Schuurmann G, Marker B, editors. Ecotoxicology: ecological fundamentals, chemical exposure, and biological effects. New York: Wiley, 1998. p. 439–50.
[12] Rainbow PS. Heavy metal in marine invertebrates. In: Furness RW, Rainbow PS, editors. Heavy metals in the marine environment. Boca Raton, FL: CRC Press, 1990. p. 67–79.
[13] Streit B. Community ecology and population interactions in freshwater systems. In: Schuurmann G, Marker B, editors. Ecotoxicology: ecological fundamentals, chemical exposure, and biological effects. New York: Wiley, 1998. p. 133–61.
[14] Schmitz OJ, Beckerman AP, Litman S. Functional responses of adaptive consumers and community stability with emphasis on the dynamics of plant-herbivore systems. Evol Ecol 1997;11:773–84.
[15] Spencer M, Ginzburg LR, Goldstein RA. Community-level risk assessment, food chains and bioaccumulation. Environ Prog 1997;19:90–7.
[16] Spencer M, Fisher NS, Wang WX. Exploring the effect of consumer–resource dynamics on contaminant bioaccumulation by aquatic herbivores. Environ Toxicol Chem 1999;18:1582–90.
[17] Wahlstrom E, Persson L, Diehl S. Size-dependent foraging efficiency, cannibalism and zooplankton community structure. Oecologia 2000;123:138–48.
[18] Yang HS, Ting YY. Artifical propagation and culture of abalone (*Haliotis diversicolor supertexta* Lischke). Bull Taiwan Fish Res Inst 1986;40:195–201.
[19] Karez CS, Magalhaes VF, Pfeiffer WC, Amado Filho GM. Trace metal accumulation by algae in Sepetiba Bay, Brazil. Environ Pollut 1994;83:351–6.
[20] Lotka AJ. The elements of physical biology. Baltimore: Williams & Wilkins, 1925.
[21] Volterra JL. Variazionie fluttuazioni del numero d'individui in specie animali conviventi. Mem Acad Lincei 1926;2:31–113. (Variations and fluctuations of a number of individuals in animal species living together. Translation In: Chapman RN, editor. Animal ecology. New York: McGraw Hill, 1931. p. 409–48).
[22] Holling CS. The components of predation as revealed by a study of small mammal predation of the European pine sawfly. Can Entomol 1959;91:293–320.
[23] Holling CS. Some characteristics of simple types of predation and parasitism. Entomology 1959;91:385–98.
[24] IMSL MATH/LIBRARY. FORTRAN subroutine for mathematical applications, Vols. 1 and 2. Houston, TX: Visual Numerics, 1994.
[25] Lee TM, Chang YC, Lin YH. Differences in physiological responses between winter and summer *Gracilaria tenuispitata* (Gigartinales, Rhodophyta) to varying temperatures. Bot Bull Acad Sin 1999;40:93–100.
[26] Chen JC, Lee WC. Growth of Taiwan abalone *Haliotis diversicolor supertexta* fed on *Gracilaria tenuistipitata* and artifical diet in a multiple-tier basket system. J Shellfish Res 1999;18:627–35.
[27] Shepherd SA. Studies on southern Australian abalone (genus *Haliotus*) XIX: long-term juvenile mortality dynamics. J Shellfish Res 1998;17:813–25.
[28] Box GEP, Hunter WG, Hunter JS. Statistics for experimenters: an inttroduction to design, data analysis, and model building. New York: Wiley-Interscience, 1978.
[29] Berthouex PM, Brown LC. Statistics for environmental engineers. Boca Raton, FL: Lewis Publishers, 1994.
[30] Hu ZL, Islam S. A method to evaluate the importance of interactions between land and atmosphere. Water Resour Res 1996;32:2497–505.
[31] Andres TH. Sampling methods and sensitivity analysis for large parameter sets. J Stat Comput Sim 1997;57:77–110.
[32] Grado SC, Chandra MJ. A factorial design analysis of a biomass to ethanol production system. Biomass Bioenerg 1998;15:115–24.
[33] Cryer SA, Havens PL. Regional sensitivity analysis using a fractional factorial method for the USDA model GLEAMS. Environ Modell Software 1999;14:613–24.